



CHORUS

This is the accepted manuscript made available via CHORUS. The article has been published as:

Doppler Boosted Dust Emission and Cosmic Infrared Background-Galaxy Cross-Correlations: A New Probe of Cosmology and Astrophysics

Abhishek S. Maniyar, Simone Ferraro, and Emmanuel Schaan

Phys. Rev. Lett. **130**, 041001 — Published 24 January 2023

DOI: [10.1103/PhysRevLett.130.041001](https://doi.org/10.1103/PhysRevLett.130.041001)

Doppler boosted dust emission and CIB-galaxy cross-correlations: a new probe of cosmology and astrophysics

Abhishek S. Maniyar,¹ Simone Ferraro,^{2,3} and Emmanuel Schaan^{2,3}

¹*Center for Cosmology and Particle Physics, Department of Physics,
New York University, New York, NY 10003, USA*

²*Lawrence Berkeley National Laboratory, One Cyclotron Road, Berkeley, CA 94720, USA*

³*Berkeley Center for Cosmological Physics, Department of Physics,
University of California, Berkeley, CA 94720, USA*

(Dated: December 16, 2022)

We identify a new cosmological signal, the Doppler-boosted Cosmic Infrared Background (DB-CIB), arising from the peculiar motion of the galaxies whose thermal dust emission source the cosmic infrared background (CIB). This new observable is an independent probe of the cosmic velocity field, highly analogous to the well-known kinematic Sunyaev-Zel’dovich (kSZ) effect. Interestingly, DB-CIB does not suffer from the ‘kSZ optical depth degeneracy’, making it immune from the complex astrophysics of galaxy formation. We forecast that the DB-CIB effect is detectable in the cross-correlation of CCAT-Prime and DESI-like experiments. We show that it also acts as a new CMB foreground which can bias future kSZ cross-correlations, if not properly accounted for.

I. INTRODUCTION

The kinematic Sunyaev-Zel’dovich (kSZ) effect is the shift in the energy of the Cosmic Microwave Background (CMB) photons when they undergo Thomson scattering off coherently moving electrons in the gas in galaxies, groups, and clusters [1, 2]. The kSZ signal is linear in gas density and independent of the temperature of the gas. This makes it a crucial unbiased probe of these electrons on the outskirts of halos and clusters out to high redshift which are otherwise hard to detect.

Using different techniques, the kSZ signal has been successfully measured through a combination of the CMB and galaxy survey data [e.g. 2, 12, 13]. Thus, the kSZ effect is now a well-established tool to localize the “missing baryons” which reside outside the virial radius of the galaxies in an ionized, diffuse, and cold gas known as the warm-hot intergalactic medium [2]. Apart from being a tracer of this gas, the kSZ signal is also a powerful probe of the radial velocities on large scales [e.g. 6–8]. This makes the kSZ effect a probe of dark energy [9], modified gravity [10], cosmic growth rate of structure [11], primordial non-Gaussianity of local type (f_{NL}) [12] when used in combination with other matter tracers like galaxies. These techniques, however, suffer from the well-known problem of ‘kSZ-optical depth degeneracy’ where the overall normalization of the electron profile in a halo is not known very well. So although we can measure the shape of the velocity power spectrum well with a combination of kSZ and galaxies, this degeneracy leads to an unknown overall normalization of the measured velocity field.

In this paper, we present a new observable which is very analogous to the kSZ effect but does not suffer from the ‘optical depth degeneracy’ which kSZ suffers from. This observable is the Doppler boosted emission of the cosmic infrared background (CIB), which we will call DB-CIB from here onward (Fig. 1). The CIB is cumulative

infrared emission from all the dusty star forming galaxies throughout the Universe [1]. It is an excellent probe of the cosmic star formation and the large scale structure of the Universe [14, 15].

If a galaxy contributing to the CIB has a non-zero line-of-sight peculiar velocity, its emission is Doppler boosted. The large-scale cosmic velocity field results in galaxy bulk motions, which in turn source the DB-CIB signal of interest in this paper.

Unlike kSZ, the DB-CIB does not originate from scattering CMB photons: the Doppler boosting is imprinted on the galaxy’s thermal dust emission. However, the DB-CIB signal is deeply analogous to the kSZ: it measures the product of velocities with the mean infrared luminosity. Crucially, this mean infrared luminosity can be measured independently, unlike the kSZ optical depth. It is thus ‘calibratable’ and can be removed, providing unbiased estimates of the velocity field. This is precisely the reason we do not have an analogous optical depth degeneracy here. In this paper, we compute for the first time the expected signal-to-noise (SNR) for the detection of this signal for a Planck-like [16] and Fred Young sub-millimeter telescope (CCAT-Prime) -like [17] experiment. This effect also acts as a contaminant to the kSZ measurements from the CMB power spectrum and from the cross-correlation of CMB with galaxies. We will quantify this contamination in this work.

The remainder of this paper is organized as follows. In the following Sec. II, we derive the formalism to quantify this DB-CIB emission. Then in Sec. III, we present the formalism to detect this effect through cross-correlation of the CIB with velocity-weighted density field. We then present the expected SNR of this signal for the Planck and CCAT-Prime experiments in combination with the CMASS [18] catalog from the Baryon Oscillation Spectroscopic Survey (BOSS) and the Dark Energy Spectroscopic Instrument (DESI) galaxy survey (Sec. IV). We present potential applications of this signal in Sec. V.

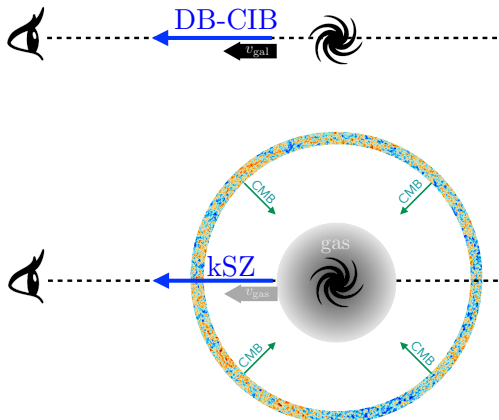


FIG. 1. Although the DB-CIB effect is analogous to the kSZ, there is a subtle difference between the two. While the kSZ pertains to the Doppler effect of the CMB photons scattering off of hot intra-cluster gas, DB-CIB is the Doppler effect on the infrared emission from a galaxy with a peculiar velocity along our line-of-sight. Thus, the kSZ is proportional to the optical depth of the hot gas τ , whereas DB-CIB is insensitive to it, and thus probes the velocity field without ‘ τ degeneracy’. In the above case, both the hot gas and galaxy are moving towards us resulting in the up-shifting of the photon energy through the kSZ and DB-CIB effect respectively.

II. DOPPLER-BOOSTED CIB EMISSION

For any specific intensity $I(\nu)$ at frequency ν , the quantity $I(\nu)/\nu^3$ is a conserved quantity under Lorentz transformations, including boosts. Using this and taking cosmological expansion into account, the fractional change in the specific intensity due to Doppler boosting is

$$\frac{\Delta I^{\text{DB}}(\nu_0)}{I(\nu_0)} = \beta(3 - \alpha_{\nu_0}) + \mathcal{O}(\beta^2), \quad (1)$$

where $\beta = v/c \ll 1$ with v being the source peculiar velocity with respect to us and c is the speed of light, ν_0 is the observed frequency, and α_{ν_0} is the logarithmic slope of the observed intensity with respect to the observed frequency (see Eq. 5 and Fig. 1 in Suppl. Mat). A detailed derivation is presented in Suppl. Mat. I ([1–18]).

This is analogous to the kSZ effect (Fig. 1) where the fractional change in the CMB temperature due to the bulk flow motion of the hot gas comes out to be $\Delta T^{\text{kSZ}}/T \propto \tau\beta$ where τ is the optical depth of the hot gas which is not known a priori. Peculiar velocity field measurements using the kSZ therefore suffer from the ‘kSZ-optical depth degeneracy’. For the DB-CIB effect on the other hand, all the terms are *calibratable*, as we shall see, and there is no such degeneracy.

Importantly, the equation so far applies to *any* emission process, including infrared emission giving rise to the CIB, but also synchrotron emission and any other radiative process across the whole electromagnetic spectrum. In what follows, we shall study the case of the

CIB in detail, since the CIB dominates the extragalactic emission at millimeter and sub-millimeter frequencies. For the CIB, $I^{\text{obs}}(\nu_0)$ can be calculated using Eq. (14), details of which are provided in Suppl. Mat. III. This requires a prior knowledge of the effective spectral energy distribution (SED) $S_{\nu_0}^{\text{eff}}(z)$ of the Infrared (IR) galaxies at a given redshift and frequency. We use the $S_{\nu_0}^{\text{eff}}(z)$ templates from a stacking analysis presented in [6]. An alternative approach in [1] fits for $S_{\nu_0}^{\text{eff}}(z)$ with a modified blackbody parameterization such that $S_{\nu_0}^{\text{eff}}(z) \propto \nu_0^{\beta_d} B_{\nu_0}(T_d(z))$ where B_{ν_0} denotes the Planck function, T_d denotes the dust temperature as a function of redshift, and β_d is the emissivity index encoding information about the physical nature of the dust. In Fig. 1, we show α_{ν_0} as a function of the observed frequency and redshift for these two choices of SEDs. Looking at Eqs. (1) or (6), we see that the DB-CIB emission is proportional to a factor of $(3 - \alpha_{\nu_0})$. We find that $\alpha_{\nu_0} \approx 3$ for frequencies between ~ 100 -500 GHz for different redshifts when we use SEDs from [6]. Thus, the Doppler-boosted signal might be reduced for these choices of frequencies. Interestingly, the spectral index α_{ν_0} becomes negative at high frequencies. This indicates a drop-off of intensity with respect to the observed frequency, when observing above 1.5-2.5 THz depending on the model and the redshift of the source. Since the factor of $(3 - \alpha_{\nu_0})$ is increased for negative α_{ν_0} , the Doppler boosting of the CIB is more prominent at higher frequencies.

At very low frequencies ($\nu < 70$ GHz) where we expect the CIB intensity to drop-off, template SEDs from [6] instead flatten out, leading to $\alpha_{\nu_0} \approx 0$ in this case. At such low frequencies, synchrotron radiation coming from extragalactic sources compensates for the drop in the infrared emission making the final intensity almost constant with frequency which results in $\alpha_{\nu_0} \approx 0$. While this effect is included in the template SEDs from [6], it is not included in the modified blackbody template shown in the dashed curves and therefore the value of α_{ν_0} differs between the two SEDs at these low frequencies. The synchrotron radiation itself is also Doppler boosted, allowing us to treat it with the same formalism.

III. CROSS-CORRELATION WITH GALAXIES

The DB-CIB signal is too small to be detected at the power spectrum level as we show in Suppl. Mat. VI. To detect this effect, we rely on two facts: 1– along with the kSZ, DB-CIB is the only other component correlated with velocities and 2– at high frequencies where CIB dominates and the kSZ contribution is negligible (see Sec. IV). Thus, our approach to the DB-CIB detection follows the kSZ detections by [2, 13], who stacked the ACT CMB maps, appropriately weighted by an external tracer of peculiar velocity, at the positions of the BOSS galaxies. Here we propose a similar procedure through cross-correlation of the observed raw map at high frequencies (where CIB dominates) with a density-weighted

velocity field (momentum) $\mathbf{q}(\mathbf{x})$ from the galaxy positions.

In the Limber and flat sky approximations, the angular cross-power spectrum of the fluctuations in the raw high frequency map $\Delta I(\nu_0)$ and the line of sight component of $\mathbf{q}(\mathbf{x})$ i.e. $q_\gamma(\mathbf{x})$ is

$$C_\ell^{\Delta I_{\nu_0}^{\text{DB}} q_\gamma} = \int \frac{d\chi}{\chi^2} W^{\Delta I_{\nu_0}}(\nu_0, z) W^q(z) P^{\Delta I_{\nu_0} q_\gamma} \left(\frac{\ell + 1/2}{\chi}, z \right), \quad (2)$$

where χ is the comoving distance to redshift z , $W^{\Delta I_{\nu_0}}(\nu_0, z)$ and $W^q(z)$ are the window functions corresponding to the CIB fluctuations and the galaxy survey, respectively. $P^{\Delta I_{\nu_0} q_\gamma} \left(\frac{\ell + 1/2}{\chi}, z \right)$ is the cross-power spectrum of the fluctuations in the raw map and the line-of-sight component q_γ which is given as

$$P^{\Delta I_{\nu_0} q_\gamma}(k, z) = (3 - \alpha_{\nu_0}) P^{\Delta I_{\nu_0} \delta_g}(k, z) \langle \beta_{\text{LOS}}^2 \rangle(z), \quad (3)$$

where $\langle \beta_{\text{LOS}}^2 \rangle(z)$ is the variance of the line of sight velocity and $P^{\Delta I_{\nu_0} \delta_g}(k, z)$ is the cross-power spectrum of the CIB fluctuations and the galaxy overdensity field. A detailed derivation is provided in Suppl. Mat. II.

Eq. 3, together with Eq. 2 and the approximation in Eq. 9 (Suppl. Mat. II) represent the main result of this paper. The last ingredient needed to evaluate the expected signal is the cross-correlation between CIB fluctuations and galaxies, $P^{\Delta I_{\nu_0} \delta_g}(k, z)$. We calculate this cross power spectrum following the CIB halo model from [4] and the details are provided in Suppl. Mat. III. From Eq. (3), we can see that three points which make DB-CIB non-zero and detectable in cross-correlation with the momentum field are: non-zero velocities of galaxies ($\beta \neq 0$), the correlation between the galaxies in our spectroscopic catalog and the galaxies which emit the CIB ($P^{\Delta I_{\nu_0} \delta_g}$), and the frequency-dependence of the CIB, which avoids $\alpha_{\nu_0} = 3$.

IV. FORECASTS

Here we present the signal-to-noise (SNR) ratio for the cross-correlation of the raw frequency map with the momentum field. While $C_\ell^{\Delta I_{\nu_0}^{\text{DB}} q_\gamma}$ is the signal we are after, the noise includes all the components in the raw frequency map. In practice however, at the high frequencies we consider, the CIB and detector noise dominate. As a result, the SNR is calculated as

$$\left(\frac{S}{N} \right)^2 = f_{\text{sky}} \sum_{\ell_{b\text{min}}}^{\ell_{b\text{max}}} \frac{(2\ell_b + 1) \Delta \ell \left(C_{\ell_b}^{\Delta I_{\nu_0}^{\text{DB}} q_\gamma} \right)^2}{\left(C_{\ell_b}^{\Delta I_{\nu_0}^{\text{DB}} q_\gamma} \right)^2 + C_{\ell_b}^{\Delta I_{\nu_0} \Delta I_{\nu_0}} \times C_{\ell_b}^{q_\gamma q_\gamma}}, \quad (4)$$

where

$$C_{\ell_b} = \frac{1}{\Delta \ell} \sum_{\ell \in [\ell_1, \ell_2]} C_\ell, \quad (5)$$

and $\Delta \ell$ is the bin width.

$C_{\ell_b}^{\Delta I_{\nu_0} \Delta I_{\nu_0}}$ is the total binned CIB auto power spectrum at frequency ν_0 i.e. it is the sum of the one-halo, two-halo and the shot-noise power spectra, $C_{\ell_b}^{\Delta I_{\nu_0} \Delta I_{\nu_0}} = C_{\ell_b, 1h}^{\Delta I_{\nu_0} \Delta I_{\nu_0}} + C_{\ell_b, 2h}^{\Delta I_{\nu_0} \Delta I_{\nu_0}} + C_{\ell_b, \text{shot}}^{\Delta I_{\nu_0} \Delta I_{\nu_0}}$. We also add a detector white-noise term N_ℓ^{det} to this for various experiments described below. $C_{\ell_b}^{q_\gamma q_\gamma}$ is the galaxy radial velocity field power spectrum. It is obtained from $P^{q_\gamma q_\gamma}(k, z) = P^{\delta_g \delta_g}(k, z) \langle \beta_{\text{LOS}}^2 \rangle(z)$, following Eq. (3).

As previously mentioned, we use a halo model approach to calculate all the auto- and cross-power spectra, with full details in Suppl. Mat. III. Similar to the case of the CIB, for the galaxy auto- and CIB \times galaxy cross-power spectra, we sum up the 1-halo, 2-halo, and shot noise power spectrum contributions. For the CIB \times galaxy power spectra, we estimate the cross-shot noise term for a given frequency as

$$C_{\ell_b, \text{shot}}^{\Delta I_{\nu_0} \delta_g} = \sqrt{C_{\ell_b, \text{shot}}^{\Delta I_{\nu_0} \Delta I_{\nu_0}} \times C_{\ell_b, \text{shot}}^{\delta_g \delta_g}}. \quad (6)$$

In practice, this is an upper limit to the cross-shot noise term, as it assumes that the shot noise of CIB and galaxies are perfectly correlated. Since the actual level of cross-shot noise is uncertain, we only include it when forecasting the CIB SNR, not the DB-CIB SNR. Perhaps counterintuitively, this choice is actually conservative, and can only lead to underestimating the DB-CIB SNR. Indeed, the cross-shot noise is both part of our signal and noise (via its cosmic variance), but the noise contribution is negligible, since we are far from cosmic variance limited. Formally, this can be seen from Eq. (4), where the cross-shot noise term appears both in the numerator and the denominator. However, in the denominator, the cross-power spectrum is small compared to the product of the auto spectra, in our noise dominated regime. As a result, including the cross-shot noise would have no effect on the noise, but would enhance the signal. This enhanced signal will mostly be seen on very small scales ($\ell \gtrsim 3000$).

For the CIB part, we assume two different setups which correspond to Planck-like and CCAT-Prime-like experiments. For the galaxy survey, we assume four different galaxy samples corresponding to the CMASS-like ($0.44 < z < 0.70$), DESI-ELG-like ($0.0 < z < 2.0$), DESI-LRG-like ($0.0 < z < 1.4$), and extended DESI-ELG-like ($0.0 < z < 4.0$ and denoted as Ext. DESI-ELG) galaxy samples. Ext. DESI-ELG is assumed to be a hypothetical galaxy survey which detects the same number of galaxies as DESI-ELG survey, but extended over twice the redshift range. To calculate the galaxy and CIB \times galaxy power spectra within a halo model framework, a halo occupation distribution (HOD) is required. Here we use the HOD corresponding to the CMASS survey developed by [33]. We use the same HOD parametrization for the DESI-ELG, DESI-LRG, and Ext. DESI-ELG samples as well with a minor tweak: we adjust the minimum galaxy mass detectable for different samples such that the total numbers of galaxies detected by these surveys match

the expected numbers from these surveys. While not exact, this should be a reasonable approximation for our purposes. The sky fraction is assumed to be $f_{\text{sky}} = 0.4$.

Our assumed experimental setups which correspond to the Planck-like and CCAT-Prime-like experiments are given in Tab. I. The Gaussian random noise of the detector is calculated as

$$N_{\ell}^{\text{det}} = (\Delta_T)^2 e^{\ell(\ell+1)\sigma^2/8 \ln 2} \quad (7)$$

where Δ_T denotes the white noise of the detector in $\mu\text{K-arcmin}$ or Jy/sr , and σ is the full width at half maximum (FWHM) of the beam in radians. As shown in [15, 34], galactic dust dominates over the CIB power spectra below $\ell \sim 100$, and therefore we choose $\ell_{\text{min}} = 100$ in Tab. I.

Experiment	ℓ_{min}	ℓ_{max}	Δ_T $\mu\text{K-arcmin}$	σ arcmin
Planck (545 GHz)	100	5000	1137.0	4.7
Planck (857 GHz)	100	5000	29075.0	4.3
CCAT-prime (410 GHz)	100	50000	372.0	0.5
CCAT-prime (850 GHz)	100	50000	5.7×10^5	0.2

TABLE I. Experimental specifications used in this work. Planck and CCAT-Prime specifications are taken from [16] and [17]. The detector noise is quoted in thermodynamic differential CMB temperature units.

Figure 2 shows $C_{\ell}^{\Delta I_{\nu_0}^{\text{DB}} q_{\gamma}}$ for a CCAT-Prime-like 850 GHz map and DESI-ELG-like map with error bars. Our predictions for the expected SNR on the $C_{\ell}^{\Delta I_{\nu_0}^{\text{DB}} q_{\gamma}}$ for the experimental specifications considered here are given in Tab. II. Forecasts for $C_{\ell}^{\Delta I_{\nu_0}^{\text{DB}} \delta_g}$ are presented in the Suppl. Mat. III in Tab. I. As an in-depth study of the flux-cut limits for CCAT-Prime is beyond the scope of this paper, we consider two limiting cases: (i) shot noise for CCAT-Prime is equal to the shot-noise for Planck and (ii) CCAT-Prime has 10 times lower shot-noise than Planck. While the 3rd column in Tab. I and II corresponds to case (i), the 4th column corresponds to case (ii) for CCAT-Prime experiment.

As can be seen from these tables, $C_{\ell}^{\Delta I_{\nu_0}^{\text{DB}} \delta_g}$ can be detected to very high SNR. On the other hand, the DB-CIB signal $C_{\ell}^{\Delta I_{\nu_0}^{\text{DB}} q_{\gamma}}$ detection will be challenging with a Planck-like experiment considered here. A combination of CCAT-prime and DESI surveys should be able to detect $C_{\ell}^{\Delta I_{\nu_0}^{\text{DB}} q_{\gamma}}$ with a high (> 5) SNR for 850 GHz channel.

The CMASS, DESI, and Ext. DESI surveys considered here trace galaxies around redshifts ~ 0.5 , ~ 1.0 , and ~ 2.0 respectively. Therefore, SNR for $C_{\ell}^{\Delta I_{\nu_0}^{\text{DB}} \delta_g}$ for Planck is higher with 857 GHz channel than 545 GHz channel as for the CIB higher frequencies trace relatively lower redshifts and vice-versa [e.g. 14]. However, this

	Galaxy exp	DB-CIB SNR	
		High shot	Low shot
Planck 545 (857) GHz	CMASS	0.05 (0.37)	
	DESI-ELG	0.98 (5.03)	
	DESI-LRG	0.35 (3.66)	
	Ext. DESI-ELG	1.75 (5.67)	
CCAT-Prime 410 (850) GHz	CMASS	0.01 (2.30)	0.01 (2.35)
	DESI-ELG	3.71 (51.77)	4.36 (52.82)
	DESI-LRG	1.96 (31.27)	2.32 (31.93)
	Ext. DESI-ELG	15.21 (68.42)	18.00 (69.85)

TABLE II. SNR for $C_{\ell}^{\Delta I_{\nu_0}^{\text{DB}} q_{\gamma}}$ different configurations considered here. For CCAT-Prime-like experiment considered here, in the 3rd column we assume shot noise to be equal to shot noise from Planck for corresponding frequency, while in the 4th column shot noise for CCAT-Prime is 10 times smaller than Planck. Unbracketed and bracketed numbers show SNR at 545 and 857 GHz respectively for Planck, and at 410 and 850 GHz respectively for CCAT-Prime.

is not the case for CCAT-Prime experiment where SNR is lower for 850 GHz than 410 GHz. This is mainly due to the significant higher instrumental noise at 850 GHz than 410 GHz. The logic applied here has to be slightly modified while looking at Tab. II for SNR on $C_{\ell}^{\Delta I_{\nu_0}^{\text{DB}} q_{\gamma}}$. As we can see from Eq. (12), calculation of $C_{\ell}^{\Delta I_{\nu_0}^{\text{DB}} q_{\gamma}}$ from $C_{\ell}^{\Delta I_{\nu_0}^{\text{DB}} \delta_g}$ involves extra factors of $(3 - \alpha_{\nu_0})$ and $\langle \beta_{\text{LOS}}^2 \rangle(z)$ which depend on frequency and redshift respectively. The factor of $(3 - \alpha_{\nu_0})$ is smaller at 545 (410) GHz than at 857 (850) GHz (Fig. 1). Also, for the redshifts considered here, $\langle \beta_{\text{LOS}}^2 \rangle(z)$ decreases with increasing redshifts. Combining these two things again with the fact that CIB at higher frequencies traces galaxies at lower redshifts, we can see that SNR for $C_{\ell}^{\Delta I_{\nu_0}^{\text{DB}} \delta_g}$ and $C_{\ell}^{\Delta I_{\nu_0}^{\text{DB}} q_{\gamma}}$ is higher at 857 (or 850) GHz than at 545 (or 410) GHz for Planck (or CCAT-Prime) experiment considered here. We note that in this calculation we use the actual redshift range corresponding to our galaxy samples to calculate α_{ν_0} unlike what we show in Fig. 1, where α_{ν_0} is calculated after integrating the CIB emission between $0 < z < z_s$ for different source redshifts z_s .

For the extended DESI-ELG like survey considered here, we see that both $C_{\ell}^{\Delta I_{\nu_0}^{\text{DB}} \delta_g}$ and $C_{\ell}^{\Delta I_{\nu_0}^{\text{DB}} q_{\gamma}}$ are detected at higher SNR than other surveys. In the case of $C_{\ell}^{\Delta I_{\nu_0}^{\text{DB}} \delta_g}$ this is solely due to obtaining the signal over a larger range of redshift (thus larger overlap with CIB redshifts [14]) compared to other surveys. As can be seen from Fig. 1, the value of α_{ν_0} is lower when galaxies over a broad redshift range (e.g. Ext. DESI-ELG: $0 < z < 4$) are considered compared to a narrower range (e.g. DESI-ELG: $0 < z < 2$). This results in a higher value of the $(3 - \alpha_{\nu_0})$ factor which enters in the calculation of $C_{\ell}^{\Delta I_{\nu_0}^{\text{DB}} q_{\gamma}}$

for surveys of broader redshift range. Combined with the larger redshift overlap with the CIB, this effect adds to have higher SNR for $C_\ell^{\Delta I_{\nu_0}^{\text{DB}} q_\gamma}$ detection with Ext. DESI-ELG survey compared to other surveys.

The SNR in case (ii) for CCAT-Prime experiment in Tab. I is smaller than in case (i) which has a higher shot noise compared to former. This is because the cross-shot noise term given in Eq. 6, adds to the signal for CIB \times galaxy cross-correlation. This is not the case for $C_\ell^{\Delta I_{\nu_0}^{\text{DB}} q_\gamma}$ where there is no cross-shot noise term in Eq. 4 and only the auto-shot power spectrum for the CIB and galaxy survey appear in the denominator acting as noise decreasing the SNR. Therefore, unlike for CIB \times galaxy, the SNR slightly increases for case (ii) compared to case (i). In other words, unlike for the case of CMB observations where decreasing foreground levels by masking sources is beneficial, in our case the Doppler-boosted emission from the sources *is* our signal, and therefore aggressive masking is not guaranteed to lead to higher SNR. In fact, more aggressive masking will reduce the noise (by reducing shot noise), but will also reduce the signal. A full study of the optimal flux cuts that maximize the SNR is beyond the scope of this paper.

V. DISCUSSION AND CONCLUSIONS

Emission coming from the CIB galaxies gets boosted by the Doppler effect as a result of their motion in the large scale cosmological velocity field. In this paper, we present a formalism to calculate this effect and quantify the detectability of the cross-correlation of the CIB with a velocity weighted galaxy density field. We show that although this effect would be hard to detect through a cross-correlation of Planck and CMASS/DESI galaxies, a combination of the CCAT-Prime and DESI survey can potentially detect this signal.

We show that the kSZ effect acts as a bias to the DB-CIB measurement and vice-versa i.e. the DB-CIB constitutes a new source of foreground while measuring the kSZ power spectrum, and a bias to stacking-based kSZ estimators (Suppl. Mat. IV, V, and VI). For upcoming CMB experiments like SO and CMB-S4 which plan to detect the kSZ at a very high significance, this foreground contamination will have to be considered and removed. We point out in Suppl. Mat. V, this can be done using the distinct frequency dependence, as well as the different

angular profile of this effect.

As mentioned in Sec. I, the radial velocity field is an excellent cosmological probe. It has been shown that the kSZ tomography technique can be successfully used to measure the radial velocity field with the upcoming CMB surveys [8, 12]. Due to the ‘kSZ optical depth degeneracy’, the overall normalization of the measured velocity is not known a priori and must be marginalized over. This is not an issue for measurements of f_{NL} due to the scale dependence of the signal, but it poses a significant challenge for measurements that require knowledge of the normalization, such as growth of structure which depend on the amplitude of the velocity power spectrum.

From Eq. (3), we can see that the DB-CIB emission can act a new observable to reconstruct the velocity field β , free from this degeneracy. Thus, we can construct an estimator for β using a combination of a CIB and galaxy survey or solely using the CIB. This estimator has an advantage over the kSZ tomography technique as it does not suffer from the ‘optical depth degeneracy’ as the intensity of the CIB emission at a given frequency I_ν is *calibratable* by direct measurement of the cross-correlation $C_\ell^{\Delta I_{\nu_0} \delta_g}$ (or by stacking). As can be seen from Table I, the SNR on $C_\ell^{\Delta I_{\nu_0} \delta_g}$ is always a lot greater the SNR of the DB-CIB signal, so that the uncertainty on the calibration is always subdominant and should not limit the inference of the velocity field.

Thus, the velocities detected through such a technique will be a useful cosmological probe. In fact, it has to be noted that such an effect of Doppler boosting is not limited to the CIB emitting galaxies and is generalizable to any galaxy population. Therefore, such a formulation can be used with the galaxies detected through the powerful upcoming surveys like DESI, Euclid and Roman Space Telescope. In an upcoming paper, we will present such an estimator of velocity and its predictions for cosmological constraints.

ACKNOWLEDGMENTS

We thank Neal Dalal, Jacques Delabrouille, Colin Hill, Anthony Pullen and David Spergel for useful conversations. SF is supported by the Physics Division of Lawrence Berkeley National Laboratory. ES is supported by the Chamberlain fellowship at Lawrence Berkeley National Laboratory.

-
- [1] R. A. Sunyaev and Y. B. Zeldovich, Comments on Astrophysics and Space Physics **4**, 173 (1972).
 - [2] R. A. Sunyaev and Y. B. Zeldovich, MNRAS **190**, 413 (1980).
 - [3] E. Schaan *et al.*, Phys. Rev. D **93**, 082002 (2016).
 - [4] E. Schaan and Atacama Cosmology Telescope Collaboration, Phys. Rev. D **103**, 063513 (2021).
 - [5] A. Kusiak *et al.*, Phys. Rev. D **104**, 043518 (2021).
 - [6] P. Zhang, MNRAS **407**, L36 (2010).
 - [7] A.-S. Deutsch *et al.*, Phys. Rev. D **98**, 123501 (2018).
 - [8] K. M. Smith *et al.*, arXiv e-prints arXiv:1810.13423 (2018).
 - [9] S. DeDeo, D. N. Spergel, and H. Trac, arXiv e-prints astro (2005).

- [10] E.-M. Mueller, F. de Bernardis, R. Bean, and M. D. Niemack, *ApJ***808**, 47 (2015).
- [11] D. Alonso, T. Louis, P. Bull, and P. G. Ferreira, *Phys. Rev. D***94**, 043522 (2016).
- [12] M. Münchmeyer *et al.*, *Phys. Rev. D***100**, 083508 (2019).
- [13] Planck Collaboration *et al.*, *A&A***571**, A30 (2014).
- [14] A. S. Maniyar, M. Béthermin, and G. Lagache, *A&A***614**, A39 (2018).
- [15] A. Maniyar, G. Lagache, M. Béthermin, and S. Ilić, *A&A***621**, A32 (2019).
- [16] Planck Collaboration *et al.*, *A&A***571**, A6 (2014).
- [17] S. K. Choi *et al.*, *Journal of Low Temperature Physics* **199**, 1089 (2020).
- [18] C. P. Ahn *et al.*, *Astrophys. J. Suppl.* **211**, 17 (2014).
- [19] C.-P. Ma and J. N. Fry, *Phys. Rev. Lett.***88**, 211301 (2002).
- [20] A. Maniyar, M. Béthermin, and G. Lagache, *A&A***645**, A40 (2021).
- [21] J. Tinker *et al.*, *ApJ***688**, 709 (2008).
- [22] M. Béthermin *et al.*, *A&A***573**, A113 (2015).
- [23] J. L. Tinker and A. R. Wetzel, *ApJ***719**, 88 (2010).
- [24] J. L. Tinker *et al.*, *ApJ***724**, 878 (2010).
- [25] A. Cooray and R. Sheth, *Phys. Rep.***372**, 1 (2002).
- [26] S. Ferraro *et al.*, *Phys. Rev. D* **94**, 123526 (2016).
- [27] J. C. Hill *et al.*, *Phys. Rev. Lett.* **117**, 051301 (2016).
- [28] N. Battaglia, S. Ferraro, E. Schaan, and D. Spergel, *JCAP* **11**, 040 (2017).
- [29] P. Ade *et al.*, *JCAP* **02**, 056 (2019).
- [30] K. Abazajian *et al.*, arXiv e-prints (2019).
- [31] L. D. Shaw, D. H. Rudd, and D. Nagai, *Astrophys. J.* **756**, 15 (2012).
- [32] F. McCarthy and M. S. Madhavacheril, *Phys. Rev. D***103**, 103515 (2021).
- [33] S. More *et al.*, *ApJ***806**, 2 (2015).
- [34] D. Lenz, O. Doré, and G. Lagache, *ApJ***883**, 75 (2019).